Eur. Phys. J. Special Topics **229**, 3033–3042 (2020)

https://doi.org/10.1140/epjst/e2020-000070-y

THE EUROPEAN PHYSICAL JOURNAL SPECIAL TOPICS

Regular Article

Suppression of self-oscillations and formation of heterogeneous structures by diffusion in the non-linear glycolytic model

Irina Bashkirtseva[a] and Alexander Pankratov

Ural Mathematical Center, Ural Federal University, Lenina avenue, 51, Ekaterinburg 620000, Russia

Received 22 April 2020 / Accepted 9 September 2020
Published online 19 November 2020

Abstract. A dynamical distributed model of glycolysis with the diffusion is considered in the parametric zone of self-oscillations. A phenomenon of the diffusion-induced suppression of self-oscillations is found and studied by technique of harmonic coefficients. We show how, under increase of diffusion, temporal oscillations of homogeneous solutions transform into stationary non-homogeneous structures in the form of patterns-attractors. A phenomenon of multistability in this spatially distributed glycolytic model is discussed and a variety of coexisting patterns and their amplitude characteristics is quantified.

1 Introduction

The study of processes of pattern formation, initiated by seminal paper of Turing [1], attracts attention of a wide community of researchers in various fields of science [2–8]. An understanding of the basic mechanisms of self-organization in complex spatial nonlinear systems with diffusion can be achieved by developing analytical and numerical computer approaches [9–12]. Most of the research is devoted to the analysis of pattern formation in the parametric zones, where diffusion makes equilibrium homogeneous solutions unstable. Nevertheless, undoubted interest is attracted by the question of how diffusion affects self-oscillating regimes [13–15].

Processes of self-organization in glycolysis are actively studied. A generation of spatial waves in the glycolytic system was predicted in [16]. An experimental confirmation of self-organization in yeast extracts was presented in [17–19]. Mechanisms of pattern formation in glycolysis were studied on the basis of appropriate mathematical models in [20–22].

One of the first mathematical models explaining the nature of glycolytic oscillations was suggested by Higgins [23]. Using this conceptual model, it was shown that the transition from equilibrium to oscillatory mode is associated with Hopf bifurcation. A spatially distributed version of this model with diffusion was investigated in [24] where the phenomenon of pattern formation was studied in the parametric zone of the Turing instability. It was shown that this model is multistable and exhibits a coexistence of several nonhomogeneous wave-form spatial pattern-attractors. In the

[a] e-mail: irina.bashkirtseva@urfu.ru

presence of noise, a phenomenon of "stochastic preference" in pattern formation was revealed.

In this paper, we consider this distributed Higgins model in the parametric zone of self-oscillations, and study how diffusion can deform these oscillatory regimes. In Section 2, we give results of the bifurcation analysis and present the numerical scheme for computer simulation of spatiotemporal dynamics. In Section 3, a phenomenon of the diffusion-induced suppression of self-oscillations is revealed and studied with the help of harmonic coefficients. A transformation of self-oscillations of homogeneous solutions into stationary nonhomogeneous patterns is discussed. In Section 4, we study multistability of this spatially distributed Higgins model, and describe a variety of patterns and their amplitude characteristics.

2 Spatially distributed model of glycolysis

Consider the spatially distributed Higgins glycolytic model with diffusion

$$\begin{aligned} \dot{u} &= 1 - uv + D_u \frac{\partial^2 u}{\partial x^2} \\ \dot{v} &= pv\left(u - \frac{1+q}{q+v}\right) + D_v \frac{\partial^2 v}{\partial x^2}. \end{aligned} \tag{1}$$

This model describes a kinetics of the glycolysis on the spatial interval $0 \le x \le L$ with no-flux conditions at boundaries $x = 0$ and $x = L$:

$$\frac{\partial u}{\partial x}(t,0) = \frac{\partial u}{\partial x}(t,L) = \frac{\partial v}{\partial x}(t,0) = \frac{\partial v}{\partial x}(t,L) = 0. \tag{2}$$

Here, functions $u(t,x), v(t,x)$ defined in $[0,+\infty) \times [0,L]$ represent concentrations of the substrate and product respectively, and parameters p and q are positive. Parameters D_u, D_v are positive diffusion coefficients.

The system (1), (2) has the homogeneous stationary solution $u \equiv 1, v \equiv 1$. In system (1) without diffusion [23], the critical value $q^* = p - 1$ corresponds to the Andronov–Hopf bifurcation: the equilibrium $(1,1)$ is stable if $q > q^*$. In the parameter zone $q < q^*$, the system (1) without diffusion exhibits self-oscillations.

In system (1) with diffusion, the critical value

$$D_u^* = \frac{q+1}{p}\left(\sqrt{q} + \sqrt{q+1}\right)^2 D_v$$

corresponds to the Turing bifurcation: the Turing instability is observed for $D_u > D_u^*$ [24].

Here and further, we fix $p = 3, D_v = 1$. For this set of parameters,

$$q^* = 2, D_u^* = (q+1)\left(\sqrt{q} + \sqrt{q+1}\right)^2/3.$$

In Figure 1, the Andronov–Hopf bifurcation border $q = q^*$ is shown by green, and Turing bifurcation border $D_u = D_u^*(q)$ is plotted by red.

In the Turing zone $q > q^*, D_u > D_u^*$, because of the diffusion instability of the homogeneous equilibrium, the system (1), (2) exhibits a phenomenon of pattern formation. This phenomenon was studied in [24] where variety of nonhomogeneous patterns-attractors was shown. It was also revealed that in the Turing instability

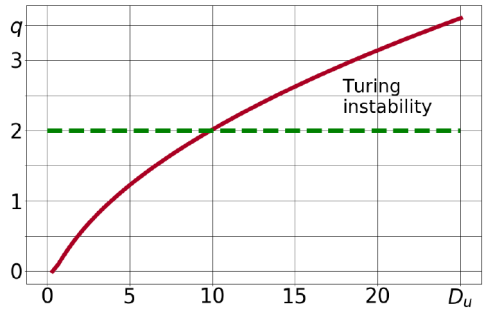

Fig. 1. Bifurcation diagram of system with $p = 3, D_v = 1$. Here, green line marks the Andronov–Hopf bifurcation, and red line is the Turing bifurcation border.

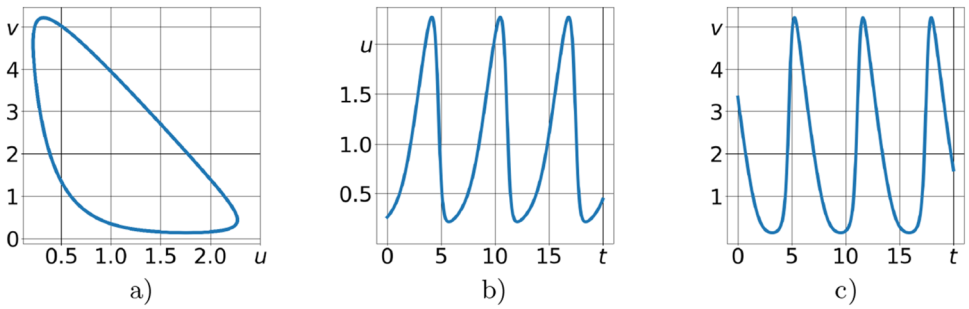

Fig. 2. Limit cycle and corresponding time series of Higgins model without diffusion for $p = 3, q = 1$.

zone, this system is multistable: for different initial states different stable patterns are generated. These patterns differ in spatial waveforms and amplitudes.

In this paper, we focus on the behavior of system (1), (2) in the parameter zone $q < q^*$ where, in absence of diffusion, the system (1) exhibits self-oscillations. An example of such oscillations is shown in Figure 2 where limit cycle and corresponding time series are plotted.

Consider now how diffusion affects these self-oscillatory modes.

For numerical analysis of system (1), (2) dynamics, we will use the explicit scheme [25] with the temporal step τ and the spatial step h:

$$\begin{aligned} u_{j+1,i} &= u_{j,i} + \tau f_{j,i} + \tau D_u \frac{u_{j,i-1} - 2u_{j,i} + u_{j,i+1}}{h^2} \\ v_{j+1,i} &= v_{j,i} + \tau g_{j,i} + \tau D_v \frac{v_{j,i-1} - 2v_{j,i} + v_{j,i+1}}{h^2}. \end{aligned} \tag{3}$$

Here,

$$t_j = j\tau, \quad x_i = ih, \quad u_{j,i} = u(t_j, x_i), \quad v_{j,i} = v(t_j, x_i),$$

$$f_{j,i} = f(u_{j,i}, v_{j,i}), \quad g_{j,i} = g(u_{j,i}, v_{j,i}),$$

$$f(u, v) = 1 - uv, \quad g(u, v) = pv\left(u - \frac{1+q}{q+v}\right).$$

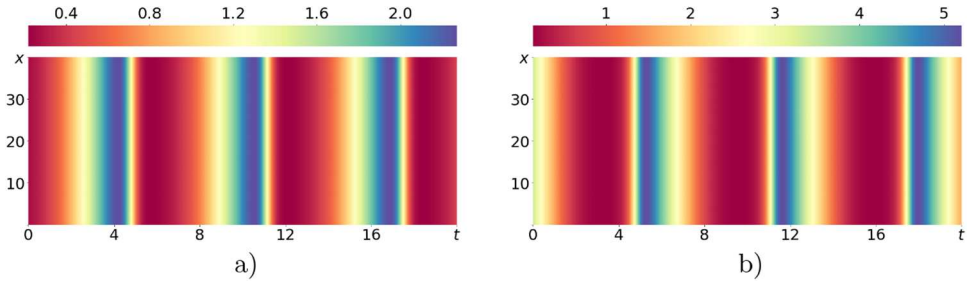

Fig. 3. Temporal periodic oscillations of homogeneous solution for $p = 3, q = 1, D_u = 5$, $D_v = 1$: (a) $u(t, x)$, (b) $v(t, x)$.

The boundary conditions (2) are approximated as follows:

$$u_{j,0} = u_{j,1}, \quad v_{j,0} = v_{j,1}, \quad u_{j,n} = u_{j,n-1}, \quad v_{j,n} = v_{j,n-1}, \qquad L = nh.$$

In our calculations, we fix $L = 40$ and use $\tau = 10^{-4}$, $h = 0.2$. For this discretization, the numerical scheme (3) is stable.

Our numerical simulations were organized as follows. We fixed a point $M(\tilde{u}, \tilde{v})$ on the limit cycle of the corresponding system without diffusion ($D_u = D_v = 0$) and started from the initial values

$$u^{\varepsilon}_{0,i} = \tilde{u} + \varepsilon\xi_i, \qquad v^{\varepsilon}_{0,i} = \tilde{v} + \varepsilon\eta_i, \tag{4}$$

where ξ_i, η_i are independent random values uniformly distributed in the interval $[-1, 1]$, and ε characterizes a magnitude of initial disturbances.

In Figure 3, we show results of numerical simulation of system (3), (4) for $p = 3$, $q = 1, D_u = 5, D_v = 1, \tilde{u} = 0.2597$, $\tilde{v} = 3.4028$, $\varepsilon = 0.1$. As one can see, here, the temporal periodic oscillations of homogeneous solution are observed. So, in presence of such diffusion, self-oscillations are preserved. Experiments show that these oscillations are stable even for increasing ε. Note that under conditions of constant homogeneity, diffusion does not actually work, and therefore the amplitude and frequency of the oscillations do not change.

3 Suppression of self-oscillations by diffusion

Under increasing parameter D_u, the behavior of the system essentially changes. In Figure 4, dynamics of the solutions is shown for $D_u = 10$. At the initial temporal stage, the system repeats several times the oscillations of the homogeneous structure. Further, these homogeneous structures are destroyed and transformed into nonhomogeneous structures with decaying time oscillations of the amplitudes. As a result, the stationary nonhomogeneous spatial pattern-attractors are formed. These stages are well seen in Figures 4a and 4c for u- and v-coordinates of solutions. Here, oscillations of the homogeneous structure continue till $t \approx 20$, further we see a stage of the destruction, and for $t > 50$, one can observe stabilization of the nonhomogeneous pattern.

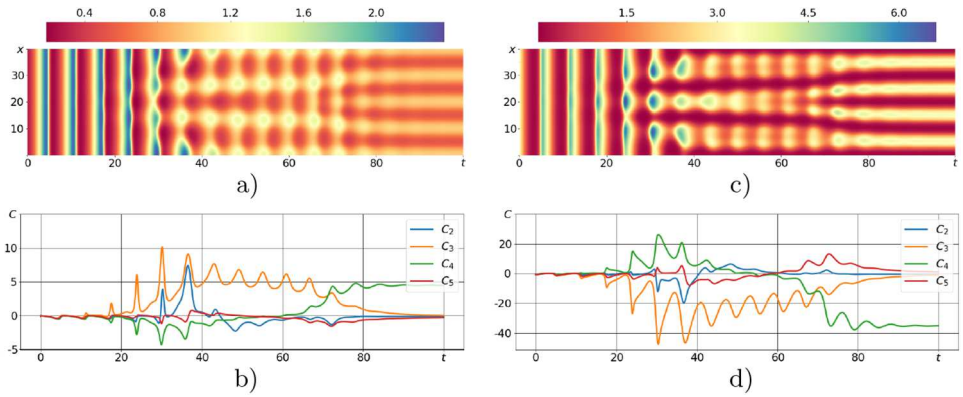

Fig. 4. System with $D_u = 10$: (a) dynamics of u-coordinate with corresponding harmonic coefficients (b); (c) dynamics of v-coordinate with corresponding harmonic coefficients (d).

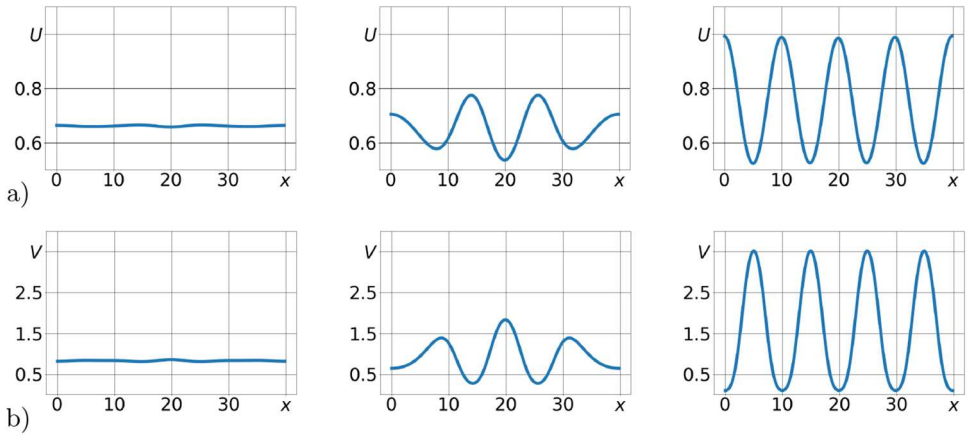

Fig. 5. System with $D_u = 10$ at $t = 8$, $t = 27$, and $t = 100$: (a) snapshots of u-coordinate of structure; (b) dynamics of v-coordinate of structure.

For detailed quantitative description of the spatiotemporal changes in the behavior of the function $\varphi(t, x)$, one can use harmonic coefficients

$$C_k(t) = \int_0^L \varphi(t, x) \cos(2\pi x k / L) dx.$$

In Figures 4b and 4d, plots of the function $C_k(t)$ are shown for $u(t, x)$ and $v(t, x)$ for several k. At the first stage, we see growth of amplitude of harmonic coefficients and dominance of C_3. At the second stage, coefficients are re-arranged, and C_4 starts to dominate. Further, the coefficient C_4 is stabilized while others vanish.

Three snapshots of this transient process are shown in Figure 5 for the variables u and v, and $t = 8$, $t = 27$, and $t = 100$.

To distinguish spatial patterns, we will use the following notations: pattern is identified by the number of peaks, and the direction $\uparrow$ or $\downarrow$, which is determined by the behavior of u-coordinates near the right border $x = L$. Note that for u and v these directions are always opposite.

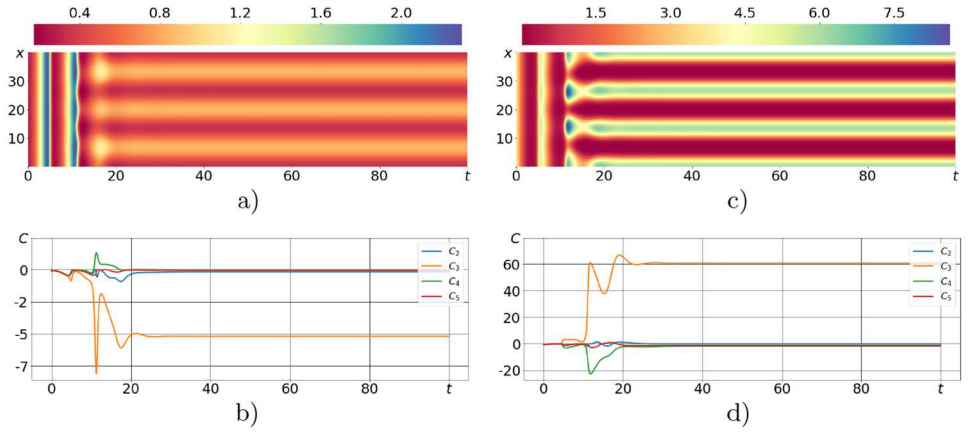

Fig. 6. System with $D_u = 20$: (a) dynamics of u-coordinate with corresponding harmonic coefficients (b); (c) dynamics of v-coordinate with corresponding harmonic coefficients (d).

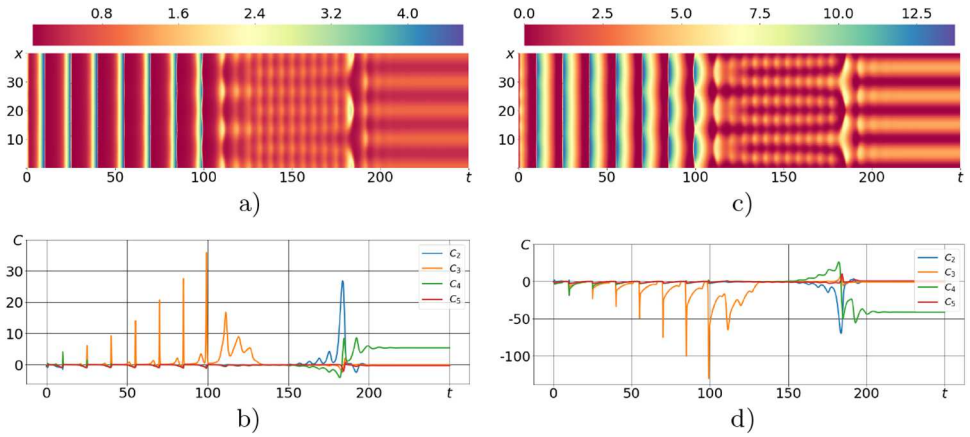

Fig. 7. Suppression of self-oscillations for $q = 0.5, D_u = 7$: (a) dynamics of u-coordinate with corresponding harmonic coefficients (b); (c) dynamics of v-coordinate with corresponding harmonic coefficients (d).

For example, in Figure 5c, we see 4 ↑-pattern. Comparing Figures 4 and 5, one can conclude that temporal dominance of C_3 at the second stage corresponds to the transient structure 3 ↑, and the stabilized C_4 corresponds to the final pattern-attractor 4 ↑. So, the dominance of the harmonic coefficient C_k signals about the prevalence of k-wave pattern.

Consider what happens under further increase of D_u. In Figure 6, transformation of self-oscillations of homogeneous structures into stationary non-homogeneous patterns are shown for $D_u = 20$. Colored diagrams of transient processes and plots of harmonic coefficients show that the increase of D_u results in the shortening the transient process.

One more example of the diffusion-induced of suppression of self-oscillations is shown in Figure 7a for $q = 0.5$ and $D_u = 7$. Here, the system exhibits a more complex transient process with transitions: homogeneous 0-pattern → 3-pattern → 6-pattern → 4-pattern. These changes in temporal dynamics, are clearly reflected by harmonic coefficients.

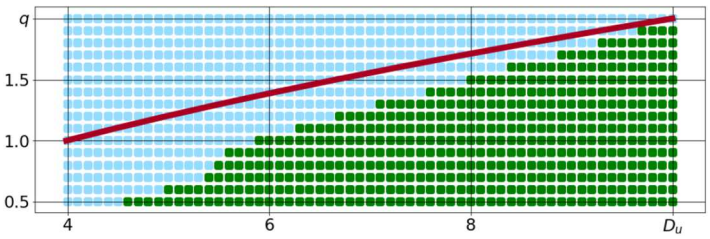

Fig. 8. Dynamical regimes of system with diffusion. Blue points mark homogeneous self-oscillations, and green points mark non-homogeneous stationary pattern formation.

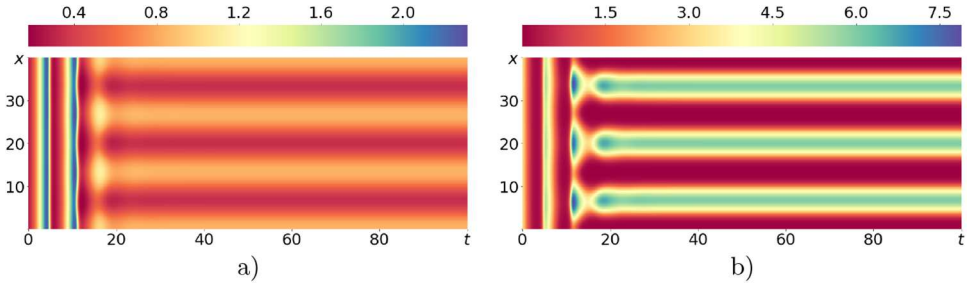

Fig. 9. System with $D_u = 20$: (a) dynamics of u-coordinate; (b) dynamics of v-coordinate. Here, another pattern is formed in comparison with Figure 6.

So, in the parameter zone $q < q^*$, self-oscillations appearing in the system without diffusion can both be preserved or destroyed by diffusion of appropriate intensity. In Figure 8, for $p = 3$ and $D_v = 1$, (D_u, q)-parametric diagram shows these two regimes. Here, blue zone corresponds to homogeneous self-oscillations, and green zone describes the diffusion-induced non-homogeneous stationary pattern formation.

4 Multistability

It is worth noting that in green zone (see Fig. 8), the system (1),(2) exhibits a wide diversity of non-homogeneous patterns-attractors. These patterns essentially differ in the quantity of spatial waves and amplitudes. Moreover, the system (1),(2) with all fixed parameters can exhibit different stationary patterns in dependence of the initial data. For example, in Figures 6 and 9, a process of pattern formation in system (1),(2) with the same set of parameters $p = 3, q = 1, D_v = 1, D_u = 20$ and slightly varying initial values results in the different final patterns. Indeed, in Figure 6 it is $3\downarrow$-pattern whereas in Figure 7 it is $4\uparrow$-pattern.

Indeed, the system (1),(2) exhibits a complex multistability with several coexisting attractors. In Figure 10, examples of some of them are shown for $D_u = 7$ and $D_u = 20$.

Zones of the existence of these patterns can be seen in Figure 11 where extremum values of spatial waves for u-coordinate are plotted versus diffusion coefficient D_u.

In our numerical simulations, we used various realizations of the random initial states (4) and observed various patterns-attractors with different probability. Results of our statistical analysis are presented in Figure 12 for three values of the diffusion coefficient D_u and 2000 samples. These results can be interpreted as the "preference of attractors." Indeed, for $D_u = 7$, patterns with 4 and 4.5 peaks are most probable. For $D_u = 10$, the system prefers patterns $4\uparrow$. For $D_u = 20$, a top list of preferences is $3\uparrow$, $3.5\downarrow$, and $3.5\uparrow$.

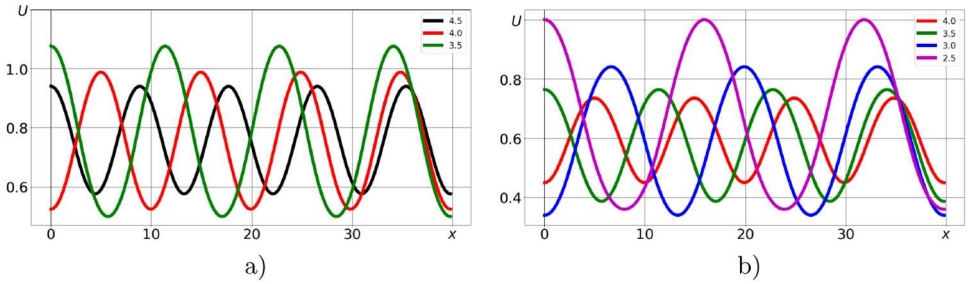

Fig. 10. Examples of patterns: (a) $D_u = 10$, (b) $D_u = 20$.

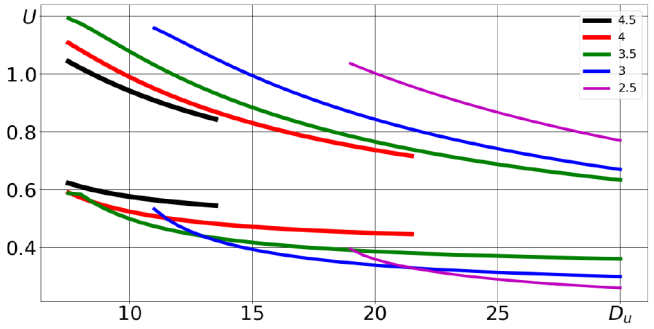

Fig. 11. Extrema of u-coordinates of stationary patterns in system (1), (2) with $p = 3$, $q = 1, D_v = 1$.

5 Conclusion

We studied the distributed glycolytic model with the diffusion. It was shown that the diffusion in this model can cause stationary nonhomogeneous patterns even in the parameter zone where initial local model (without diffusion) exhibits self-oscillations. This phenomenon of the diffusion-induced suppression of self-oscillations was studied by harmonic coefficients. We revealed that considered system is multistable with coexisting stationary patterns-attractors of different wave forms. A parametric study of amplitudes and variety of wave forms of patterns was carried out. Statistical analysis revealed the "preference" for certain types of patterns under the random variation of the initial data.

The work was supported by Russian Science Foundation (No. 16-11-10098).

Author contribution statement

I.B. and A.P. contributed to the implementation of the research, to the analysis of the results and to the writing of the manuscript.

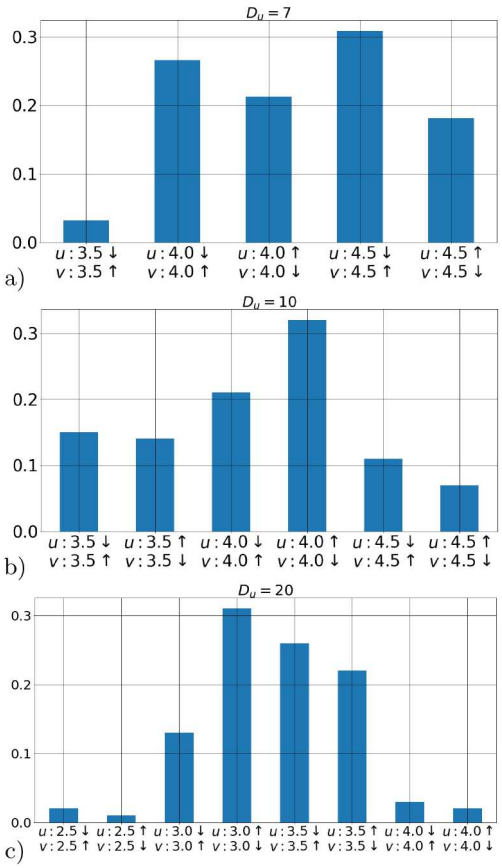

Fig. 12. Statistics of patterns: (a) $D_u = 7$, (b) $D_u = 10$, (c) $D_u = 20$.

References

1. A.M. Turing, Philos. Trans. Roy. Soc. London. Ser. B, Biol. Sci. **237**, 37 (1952)
2. G. Nicolis, I. Prigogine. *Self-organization in nonequilibrium systems* (Wiley, New York, 1977)
3. M.C. Cross, P.C. Hohenberg, Rev. Mod. Phys. **65**, 851 (1993)
4. S. Levin, Ecology **73**, 1943 (1992)
5. A.J. Koch, H. Meinhardt, Rev. Mod. Phys. **66**, 1481 (1994)
6. P. Ball, N.R. Borley, *The self-made tapestry: pattern formation in nature* (Oxford University Press, Oxford, 1999)
7. J.D. Murray, *Mathematical biology. II. Spatial models and biomedical applications* (Springer-Verlag, New York, 2001)
8. I. Bashkirtseva, A. Pankratov, E. Slepukhina, I. Tsvetkov, Philos. Trans. Roy. Soc. A: Math. Phys. Eng. Sci. **378**, 20190253 (2020)
9. G. Dangelmayr, I. Oprea, *Dynamics and bifurcation of patterns in dissipative systems* (World Scientific, 2004)
10. E. Meron, *Nonlinear physics of ecosystems* (CRC Press, Boca Raton, FL, USA, 2015)
11. A. Kolinichenko, L. Ryashko, J. Comput. Nonlinear Dyn. **15**, 011007 (2020)
12. A.P. Kolinichenko, A.N. Pisarchik, L.B. Ryashko, Philos. Trans. Roy. Soc. A: Math. Phys. Eng. Sci. **378**, 20190252 (2020)
13. T. Kohsokabe, K. Kaneko, Europhys. Lett. **116**, 48005 (2016)
14. Y. Li, J. Wang, X. Hou, J. Math. Anal. Appl. **449**, 1863 (2017)

15. T. Kohsokabe, K. Kaneko, Chaos **28**, 045110 (2018)
16. A. Goldbeter, model. Proc. Natl. Acad. Sci. U.S.A. **70**, 3255 (1973)
17. A. Boiteux, B. Hess, Berich. Bunsenges. Physikal. Chem. **84**, 392 (1980)
18. T. Shinjyo, Y. Nakagawa, T. Ueda, Physica D **84**, 212 (1995)
19. T. Mair, C. Warnke, S.C. Müller, Faraday Discuss. **120**, 249 (2001)
20. A.I. Lavrova, S. Bagyan, T. Mair, M.J.B. Hauser, L. Schimansky-Geier, BioSystems **97**, 127 (2009)
21. J. Zhou, J. Shi, IMA J. Appl. Math. **80**, 1703 (2015)
22. A. Atabaigi, A. Barati, H. Norouzi, Comput. Math. Appl. **75**, 4361 (2018)
23. J. Higgins, Proc. Natl. Acad. Sci. U.S.A. **51**, 989 (1964)
24. I. Bashkirtseva, A. Pankratov, Eur. Phys. J. B **92**, 238 (2019)
25. K.W. Morton, *Numerical solution of partial differential equations: an introduction* (Cambridge University Press, Cambridge, 2005)